FINAL SAFETY EVALUATION BY THE OFFICE OF NUCLEAR REACTOR REGULATION

TOPICAL REPORT ANP-10297P, REVISION 0

"THE ARCADIA® REACTOR ANALYSIS SYSTEM FOR PWRs

METHODOLOGY DESCRIPTION AND BENCHMARKING RESULTS"

AREVA NP, INC.

PROJECT NO. 728

1.0 INTRODUCTION

By letter dated March 31, 2010, AREVA NP, Inc. (AREVA) submitted Topical Report (TR) ANP-10297P, Revision 0, "The ARCADIA® Reactor Analysis System for PWRs [Pressurized Water Reactors] Methodology Description and Benchmark Results" (Agencywide Documents Access and Management System (ADAMS) Accession No. ML100950584), to the U.S. Nuclear Regulatory Commission (NRC) for review and approval. The application methodology and benchmarking results of the ARCADIA® code system for application to neutronic design analyses of PWRs (Reference 1) is evaluated in this draft safety evaluation (SE). In general, the presented methodology for each section was evaluated for its applicability to the intended application. Possible limitations of the proposed methodologies were also taken into consideration. The presented benchmark and validation cases were evaluated for the intended ARCADIA® code system application range as defined under Section 13 of the TR. The experimental data and benchmarks were checked for their adequacy for the intended application range.

2.0 REGULATORY EVALUATION

2.1 APOLLO2-A METHODOLOGY

APOLLO2-A is a deterministic neutronics code designed for lattice physics calculations developed by AREVA for its industrial applications. APOLLO2-A solves the 2D (two dimensional) transport equation for 281 neutron energy groups and 94 gamma energy groups using Collision Probability (CP), Integro-Differential Transport Solver (IDT) and Method of Characteristics (MOC) solution methods in stages. The main purpose of this code is to provide fuel assembly averaged microscopic cross sections heterogeneous form functions and kinetic parameters for the three-dimensional (3D) neutronics ARTEMIS™ core simulator.

As this review does not go into detail in the solution algorithm and resonance treatments, the application of the available models to generate homogenized cross sections were reviewed. A xenon equilibrium model to estimate Xe^{135} and I^{135} equilibrium concentrations for zero burnup is described under Section 2.8 Fuel Depletion. However, the TR does not mention the application of this model or if it is intended to be used as part of the standard cross section generation process. The NRC staff requested additional information (RAI) for the application of this model since use of equilibrium Xenon (Xe) would produce inaccurate cross sections for reactor startups.

AREVA's response (Reference 2) explains that the equilibrium Xe model is only used at the beginning of base depletion, Xe branch cases are used for providing cross sections for the down-stream codes. Since Xe branch cases provide the necessary cross sections under non-equilibrium conditions, this model is acceptable.

2.2 ARTEMIS™ NEUTRONIC METHODOLOGY

The ARTEMIS™ code is a steady-state/transient 3D reactor core simulator. ARTEMIS™ solves the 3D diffusion equation using assembly average microscopic cross sections generated by APOLLO2-A. ARTEMIS™ solves the 3D diffusion equation using Nodal Expansion Method (NEM) or Semi-Analytical Nodal method. Both methods are well-known industry standard methodologies used in similar codes (such as SIMULATE-3, NESTLE, AETNA02). Since the Semi-Analytical Nodal method is known to be more accurate for steep flux gradients, the semi-analytical method is the default solver mode for ARTEMIS™.

ARTEMIS™ uses a microscopic cross section model to calculate macroscopic cross sections for each solution node. After the flux solution is calculated, it performs a heterogeneous pin power reconstruction (termed dehomogenization) and provides a detailed thermal hydraulic coupling and kinetics capability.

2.2.1 Cross Section Model

ARTEMIS™ uses the common two-step approach for generating the macroscopic cross sections for the nodal solver. First, few group assembly average cross sections are generated using APOLLO2-A. The process is repeated for a base and several branch cases representing different state points. As the second step, based on the cross section model, these cross sections are interpolated for various core conditions to be used in the nodal solver.

Macroscopic cross section models are common in industry simulators. In this model, the lattice physics code provides the assembly average macroscopic cross section for various base conditions with branch perturbations. In this model, the lattice physics code, APOLLO2-A, provides the microscopic cross sections for a set of important isotopes. The simulator calculates the number densities for each node at each depletion step and calculates the macroscopic cross sections for the flux solver. Although, this model can track isotopes nodally, based on the implementation of the model, it can lose accuracy by not modeling all isotopes, neglecting history effects and multi-dimensional combinatorial effects of competing isotopes in a region. Since the details of the cross section model are not included in the TR (Reference 1), additional information was requested by the NRC staff from AREVA for clarification of the ARTEMIS™ cross section model concerns.

AREVA responded (Reference 2) by emphasizing that the ARTEMIS^{TM} cross section model is a microscopic model and the effect of a change in the microscopic cross sections on the eigenvalue is second order. AREVA also provided a sample case run showing that the current microscopic model can capture 95 percent of the history effects of an off- nominal depletion with an increased moderator temperature of 20 ^{0}K. The approach to answer the history effect concerns are acceptable, however, the effects of a 20 ^{0}K moderator temperature perturbation is not believed to be as large as other spectral effects, such as control rod history. Therefore, a similar analysis should be provided for the control rod history contribution to show the accuracy of the current implementation. In addition, AREVA did not address the concerns about deficiency in capturing the effect of isotopic neutron competition (or self-shielding) in the model in its first response. Consequently, a second RAI was sent to AREVA for more information regarding the microscopic cross section model.

AREVA responded (Reference 2) by describing the detailed tabular structure used in the microscopic cross section model. The parameterization of the microscopic model is similar in formulation to current macroscopic models, though potentially many more branch cases are required. The reconstructed cross section is formulated by lookup in potentially four 3D tables based on nodal exposure, moderator temperature and density, boron and xenon concentrations, and fuel temperature. The ranges of application for these parameters are significantly large, covering much more than typical ranges for PWR applications.

In addition, AREVA provided several examples of cross section validation (ARTEMIS^{TM} vs. APOLLO2-A) in their response. These examples are typical of cross section case matrix verification, and demonstrate an understanding of the concerns presented in the RAI. One example was provided of a combinatorial effect of multiple off-nominal conditions, which resulted in good agreement. While this example is not considered to be of a bounding level of difficulty in reconstruction, and did not include competing effects of boron or xenon on the model, AREVA provided a viable explanation in their response to address the concern.

As briefly mentioned in the TR (Section 1.0 and Section 3.5), ARTEMIS^{TM} uses a single cross section library for all moderator densities, contrary to separate cold and hot condition libraries used in other industry codes. The two operating conditions (hot and cold) typically differ by inclusion of Xenon and Doppler effects, which can create a discontinuity in the cross sections at intermediate temperatures. Therefore, unified cross section models can potentially introduce relatively higher cross section errors during the startups, shutdowns and transients. Consequently, additional information regarding the application of the unified library and its validation at cold conditions was requested by the staff from AREVA.

In their response (Reference 2), AREVA pointed to the similar methodology used in the “NEMO” (Reference 3) and “SCIENCE” (Reference 4) codes. AREVA also provided additional technical justification to validate APOLLO2-A under the cold conditions. However, the NRC staff felt that unless it can be shown that the ARTEMIS^{TM} microscopic cross section model reduces to the APOLLO2-A microscopic cross sections at cold conditions, accuracy of APOLLO2-A microscopic cross sections at cold conditions does not assure the accuracy of the ARTEMIS^{TM} cross section model. Therefore, another RAI was sent to AREVA for clarification.

In the response (Reference 2), AREVA provided a description and the range of applicability of the microscopic cross section model, which well encompasses cold conditions. Furthermore, the response also pointed out that the xenon number density is explicitly treated as a cross section parameter, and that the moderator temperature/density and fuel temperature, are each

treated completely independently. Therefore, the assumptions made for typical cold cross section libraries (isothermal, no xenon conditions) are not relevant to this model and therefore will not lead to large discontinuities or errors.

2.2.2 Pin Reconstruction

The pin power reconstruction process in ARTEMIS™ is used to estimate the pin powers from the ARTEMIS™ calculated nodal average and surface average fluxes. The ARTEMIS™ pin power reconstruction method is very similar to the methodology used in other industry codes. In this approach, the available node average flux and surface fluxes are fit to a 2D polynomial to get the homogenous flux distribution for each pin. As the second step, the calculated intra nodal homogenous fluxes are corrected with the pin by pin form factors calculated from the lattice physics code. The assumption in the second step is that the homogenous to heterogeneous pin flux ratios are constant regardless of the flux gradient in the fuel assembly.

Since detector responses are also calculated using the same methodology, accuracy of the detector responses for the fuel assemblies on the periphery are questioned. Consequently, the staff requested additional information from AREVA demonstrating the accuracy of this methodology for the peripheral fuel assemblies.

AREVA responded (Reference 2) by stating that the nodal flux polynomial fit captures the effect of the flux gradient in the fuel assembly due to flux gradients in the neighboring assemblies and therefore the methodology should be applicable in the peripheral nodes as well. AREVA's answer addresses the accuracy of the calculated homogenous intra- nodal flux in the first step. AREVA also pointed out (Reference 2) that uncertainty in pin powers due to steep flux gradients, are already captured in multi-assembly calculations. AREVA's explanation is found to be satisfactory by the NRC staff.

In this section of the TR, AREVA also discussed calculation of pin powers from the dehomogenized pin fluxes, and pin-by-pin fission power cross sections ($\kappa\Sigma_f$). In addition, a second dehomogenization procedure similar to flux dehomogenization is used to calculate pin-by-pin powers. This approach is also common in advanced core simulators.

2.2.3 Fuel Assembly Shuffling and Repository

The ARCADIA® code system includes an assembly shuffling and repository module called POSEIDON. This module is responsible for in-core fuel assembly shuffling as well as discharging fuel assemblies to the spent fuel and dry storage. POSEIDON provides tracking of all assembly inventory and fuel isotopic history. The pin power reconstruction section mentions that ARTEMIS™ calculates pin exposures by integrating reconstructed pin powers over each depletion step. This approach provides ARCADIA® pin by pin exposure tracking capability even after fuel shuffling. Since the TR doesn't mention this feature explicitly, the NRC staff requested additional information to confirm that the pin exposures are tracked throughout the life of the fuel and the pin exposures calculated by APOLLO2-A is essentially ignored in this methodology.

AREVA's response (Reference 2) confirmed that the pin exposures are shuffled and APOLLO2-A calculated exposures are ignored. AREVA's response is satisfactory since ARTEMIS™ calculated pin powers are expected to be more accurate.

2.3 ARTEMIS™ (COBRA-FLX) THERMAL-HYDRAULIC METHODOLOGY

The thermal hydraulic feedback for neutronic calculations is provided by the COBRA-FLX thermal hydraulic module in ARCADIA®. The COBRA-FLX module can perform 3D steady state and transient full core and sub-channel analyses. A variant of the well-known COBRA sub-channel code, the NRC approved code COBRA-FLX (Reference 5) solves one-dimensional (1D) axial two-phase flow equations with additional terms to account for cross flow effects. COBRA-FLX uses the power distribution from the ARTEMIS™ nodal solver to calculate core wide moderator densities and temperatures. The calculated coolant temperatures are also used by the ARTEMIS™ Fuel Rod Module to calculate fuel temperatures. Moderator density and temperature and fuel temperature are fed into ARTEMIS™ to calculate the node cross sections at a new state point. This iteration scheme is similar to other industry standard simulators.

Since the cross flow modeling is important for accident scenarios, the NRC staff requested AREVA to confirm that the effect of cross flow is indeed adequately evaluated for PWR conditions undergoing two-phase flow. AREVA confirmed (Reference 2) that the evaluation was performed for a 4 pump coast down transient in the COBRA-FLX TR (Reference 6). AREVA also provided a correction to the relevant section to prevent possible misunderstanding in the calculation flow. AREVA's response is satisfactory.

2.4 ARTEMIS™ FUEL ROD MODULE METHODOLOGY

The neutronic microscopic cross sections used in the ARTEMIS™ nodal solver are functions of temperature. The moderator temperature and density are provided by the COBRA-FLX module. The fuel rod temperatures are similarly calculated by the ARTEMIS™ Fuel Rod Module (FRM). FRM solves the 1D thermal conduction equations for static or time dependent fuel temperature profile for each fuel rod using the moderator temperature provided by COBRA-FLX. The nodal fuel temperature is represented as a single value for cross section evaluation (feedback effects). The impact of the radial temperature distribution within the pellet on the cross sections is treated by using an effective temperature model. Similar to many core simulators, an empirical effective temperature correlation is used in FRM.

The FRM proprietary effective fuel temperature model is presented without any reference or validation in the TR. Therefore, additional information was requested from AREVA regarding qualitative and quantitative technical justification of the presented correlation.

AREVA's response (Reference 2) explains that the empirical model was based on matching uranium 238 (U^{238}) capture rate in the fuel for different temperature distribution profiles. The validation studies were performed for U^{235} enrichments up to 4.40 percent and up to 60 GWD/MTU burnup. The APOLLO2-A results obtained at the effective temperature were benchmarked against Monte Carlo N-Particle (MCNP) code models with a realistic temperature profile. AREVA also points out that the empirical model used in FRM produces identical results with Rowland's formulation for steady state cases and improves the mean prediction error greatly for the transients. Rowland's formula is a well-recognized effective temperature correlation with known deficiencies in transient conditions. Based on AREVA's response and the provided references, the FRM effective fuel temperature model is well tested and acceptable.

2.5 APOLLO2-A VALIDATION

2.5.1 Introduction

Accurate simulation of the reactor core and core parameters are not possible without accurate and robust nuclear data used in the ARTEMIS™ flux solver. APOLLO2-A validation suites demonstrate the capability of APOLLO2-A to accurately model reactivity, fission rate distribution, and isotopic concentrations of a wide range of different fuel lattices.

APOLLO2-A validation methodology is based on comparisons with four cold critical experiments and spent fuel isotopic measurements. Eigenvalues and fission rate distributions from four sets of cold critical experiments are compared with APOLLO2-A calculated distributions. Additional eigenvalue comparisons are also provided from a set of cold critical integral experiments. The results from the validation are also used as one component of the pin power uncertainties calculation for the global uncertainty analyses.

2.5.2 Critical Experiments

APOLLO2-A results are compared against measurements from four sets of critical experiments shown in Table 1. The lattice configurations in these experiments vary in lattice size, fuel enrichment, void distribution, and gadolinia content.

As stated in the TR, critical experiments were modeled with the default settings in APOLLO2-A except the maximum number of flux iterations was increased in the solver. This is acceptable since the cold cases with very heterogeneous lattices are expected to converge more slowly due to increased scattering in the system.

Although APOLLO2-A results are validated against a large set of critical experiment data, all criticals presented for validation are for fresh fuel at cold conditions. Moreover, APOLLO2-A pin power uncertainties are calculated from the comparisons with these cold criticals. However, the accuracy of the calculated lattice physics parameters and hence the uncertainties can change with depletion as the fuel isotopic distribution changes. The sensitivity of the lattice physics codes to the fuel isotopic content can be due to transport models, shielding calculations, or even the raw nuclear data. The APOLLO2-A methodology and the group structure can exhibit different degrees of fidelity at different spectrums. Although fresh Mixed Oxide (MOX) fuel criticals can imitate depleted fuel behavior, highly burned fuel lattices are more challenging to model.

AREVA was requested to justify that the pin power uncertainties calculated at zero burnup cold conditions are in fact conservative. AREVA's response (Reference 2) argued that the provided critical experiments and depleted fuel isotopic comparisons should prove that the pin power uncertainties do not increase with depletion. However, the response wasn't considered satisfactory and a code to code validation with another lattice physics code was requested. Via teleconference, AREVA indicated that a previously published APOLLO2-A validation paper (Reference 7) shows APOLLO2-A depletion versus MCOR (MCNP5-KORIGEN). Based on the pin fission rate RMS comparisons of a PWR fuel assembly with 6 percent and 10 percent gadolinia content, AREVA states that many pin fission rate RMS values are between 0.2 percent and 0.4 percent, which indicates a good agreement since the MCNP sampling error is 0.3 percent (1σ).

The fission rate distribution RMS values shown in Figure 3, of Reference 7, indicates that the agreement between the two codes is around 0.3 percent at Beginning of Cycle (BOC), drops to 0.2 percent as gadolinia is depleted, and starts to increase after gadolinia is depleted reaching 0.4 percent around 80 GWd/t. It is concluded from these results that fission rate uncertainties calculated from cold criticals are not necessarily conservative when compared to all burnups. However, considering the fission rate RMS does not become greater than the value at BOC until approximately 50 GWd/t, and that assemblies at this exposure are never expected to be limiting, the BOC value calculated from the critical experiments are deemed to be acceptable.

Table 1: Cold Criticals used in APOLLO2-A Validation

Experiment	Lattice Type	U235 Enrichment	Absorber	Temp.	Void
Babcock & Wilcox	14x14-C 15x15-B 17x7-W	2.5-4.0 wt%	4.0 wt% gadolinia Pyrex, B4C, SIC	21 ^{o}C	No
KRITZ	[redacted]	[redacted]	[redacted]	[redacted]	[redacted]
EPICURE	[redacted]	[redacted]	[redacted]	[redacted]	[redacted]
CAMELEON	[redacted]	[redacted]	[redacted]	[redacted]	[redacted]

2.5.2.1 Reactivity Measurement Comparisons

The measured k-effective for each critical experiment is compared with the calculated value. The results of the comparisons show eigenvalue swings as well as biases in different directions between different sets of the same critical experiment. Although, the difference in eigenvalues is about [redacted] pcm on the average, it can change from [redacted] pcm to [redacted] pcm for the same critical experiment. Since lattice physics codes can have undesired sensitivities to geometry or isotopic distribution, this behavior can be an indication of large biases or trends to small changes in the configuration. On the other hand the different sets of the same criticals can be very different in configuration to cause such swings in eigenvalue differences. The TR does not provide any details regarding the critical experiment configurations to draw any conclusion. Therefore, AREVA was requested to provide additional information for the configuration of the critical experiments. AREVA was also requested to explain the results in the light of the differences in the configurations and provide more in-line details in the tables to allow trending or bias identification, over geometry, composition, temperature, etc.

AREVA's response (Reference 2) includes detailed descriptions of the critical experiments. Based on the number of criticals and multidimensional changes in the configuration parameters, such as temperature, boron concentration, control rod insertion, moderator void, etc., the KRITZ KWU experiments shows up to [redacted] pcm bias between the rodded and unrodded cases, the Babcock & Wilcox (B&W) experiments show a bias with increasing water rod dimensions. AREVA also reported (Reference 2) that the total uncertainty in EPICURE and CAMELON experiments is [redacted] pcm. Typical eigenvalue uncertainties in other criticals are assumed to be of the same order, that is, all eigenvalue differences are within 2σ of the experimental uncertainties. Therefore, the accuracy of APOLLO2-A results are acceptable.

2.5.2.2 Fission Rate Distribution Comparisons

Eigenvalue comparisons are based on a single calculated value for the whole lattice. Because of cancellation of errors, systematic code errors may not be discovered even with a wide range of critical experiments. On the other hand, fission rate distributions provide pin-to-pin comparisons with the experiments. Spatial accuracy of the lattice physics calculations can be evaluated and an important parameter, local pin power uncertainties, can be calculated.

Fission rate distribution comparisons are presented for the critical experiments with available fission rate distributions. The results show the RMS of relative differences in calculated to measured fission rates. Although this information is useful, just like eigenvalue comparisons, RMS can hide important details about the code accuracy at certain locations like lattice corner points, vicinity of guide tubes. As well as knowing the limiting pin power in a lattice, it is also important to know the location of the pin with the highest power accurately. Therefore, in an RAI sent to AREVA, AREVA was asked to provide fission power density distribution error maps as well as measurement errors in the critical experiments to reach a conclusion about APOLLO2-A's accuracy in pin power calculations.

AREVA provided (Reference 2) a series of available fission distribution maps and summary statistics for each comparison. The fission distribution maps show that although no relative errors exceed [redacted] percent RMS, pin to pin comparisons can be as high as [redacted] percent. In a few configurations APOLLO2-A miss-predicts the peak pin location, however, in most cases the power at the miss-predicted location is close to the peak pin power in the experiment.

It is a challenge to establish measurement uncertainties in the critical experiments. B&W 1970 criticals on the average have 1 percent uncertainty in pin fission rates. However, it can be seen in Reference 1, some pins can have as large as [redacted] percent uncertainty just from multiple measurements. As APOLLO2-A results indicate, it is clear that the more recent critical experiments have better agreements than the older ones which can be due to reduced measurement uncertainty. With a few exceptions, in general, all fission density comparisons are well within 2σ of the measurement uncertainties. The fission density comparisons show that APOLLO2-A can predict the results of the cold critical experiments very well.

2.5.3 Integral Experiments

Integral critical experiments are critical experiments with a very homogenous fuel pin configuration. Since all cells except the ones at the periphery are surrounded by similar pin cells, an integral critical experiment simulates the infinite homogenous medium conditions. Such experiments are particularly useful for validating single pin cell calculations. 1978 critical integral experiments at VALDUC facility are also used for APOLLO2-A validation. Since the current pin cell configuration is quite different than a typical PWR pin cell, the spatial resolution of APOLLO2-A model is increased to capture the increased scattering in the moderator region.

The TR mentions that in order to model the pin cell leakage, radial buckling should be taken into account as well. AREVA was asked to explain this statement along with details of the buckling treatment in APOLLO2-A. AREVA, in its response (Reference 2), explained that the axial bucklings documented in the critical experiments were used as fixed buckling in APOLLO2-A calculations. However, in integral test validations, a single pin cell is modeled in APOLLO2-A and the given buckling of the experiment accounts for the missing axial leakage and the difference between the actual radial leakage and the reflective boundary condition. The

maximum eigenvalue difference for the four different experiments with different moderator to fuel ratios is around [redacted] pcm. The results show that APOLLO2-A can model pin cells accurately.

2.5.4 Spent Fuel Analysis

Spent fuel isotopic benchmark analysis provides valuable information regarding accuracy of decay chains, depletion algorithm, and even cross section data used in a lattice physics code. Although, core simulator benchmark results would reflect the accuracy of the depletion methodology up to a degree, they can be insensitive to isotopic distributions at pin level.

In spent fuel analysis, samples from depleted fuel pins are analyzed and the measured isotopic distribution is compared with the calculated values from the lattice physics code simulation.

APOLLO2-A spent fuel analysis includes nine different experiments. The isotopic content of fuel pins from seven different power plants and two experimental cores are used for the benchmarks. A summary of the samples presented in the TR is shown in Table 2.

Table 2: Spent Fuel Analysis Benchmark Cases

Experiment	Fuel Type	Number of Samples	Enrichment	Lattice Type	Exposure (GWd/t)
Bugey	UO_2	1	3.1	17x17	25
Gravelines	UO_2	7	4.5	17x17	25, 44, 60
Malibu	UO_2	1	4.3	15x15	71
Cruas	UO_2	6	3.1,1.2	17x17	14, 22, 35
Gedeon 1	UO_2-Gd_2O_3	6	5-Gd, 3.25 U		3, 7, 11
Gedeon 2	UO_2-Gd_2O_3	6	8-Gd, 0.2 U		
Saint Laurent	MOX	7	2.9,5.6	17x17	28, 42
Dampierre	MOX	4	6.7	17x17	52, 57
Malibu	MOX	1	8.1	15x15	68

The TR only provides measured to calculated isotopic comparisons of certain isotopes of uranium (U), plutonium (Pu), and gadolinium (Gd) elements. However, for a complete assessment of the code's depletion accuracy, fission products and other major actinides should be included in the comparisons. An extended isotope list would reveal if there is any cancellation of errors or biases between certain isotopes. Moreover, unlike U and Pu isotopes, the Gd isotopes presented in the benchmark results are normalized to the total Gd concentration rather than the U^{238} concentration. The TR also doesn't specify if the calculated or measured total Gd concentration is used for normalization.

Additional details about the spent fuel analysis of APOLLO2-A and justification for Gd normalization were requested from AREVA.

In its response (Reference 2), AREVA provided detailed isotopic distribution comparisons for all validation cases. AREVA also included a simple approximation to eigenvalue contribution of each isotope to prove that isotopes with large errors do not contribute to eigenvalue calculations. Based on previous information requests for the critical experiments, available measurement and modeling uncertainties are also included. The relative errors between the

measured and the calculated isotopic concentrations are all in acceptable range. The concentrations of important reactivity contributors such U^{235}, Pu^{239}, Pu^{240}, Pu^{241}, and americium 241 (Am^{241}) are well predicted by APOLLO2-A. Based on the uncertainty estimates provided, relatively high Am^{241} errors in UO_2 samples are acceptable. In all cases APOLLO2-A results are within 2σ of the total uncertainties. AREVA also clarified use of total Gd concentrations for normalization in the UO_2-Gd_2O_3 cases by stating that the total Gd refers to total initial Gd concentration measured final U^{238} concentration is not available for a consistent normalization.

The presented spent fuel validation cases shows that APOLLO2-A can accurately deplete and track fuel isotopics from low burnups to high burnups.

2.5.5 Gamma Deposition Model

On the average, 12 percent of a fuel rod's power is a result of gamma energy deposition. Therefore, gamma energy is an important part of the pin power calculations, especially for lattices with some non-uniformity. After neutron calculations are completed and a converged flux solution is obtained, the prompt gamma sources from fission, radiative capture, and inelastic scattering and delayed gammas from fission products are calculated. Since photons can travel longer distances than neutrons before they are absorbed, accurate modeling of gamma transport is as important as accurate calculation of gamma sources in a fuel lattice. A class of approximations known as gamma smearing models has been popular in the past. The gamma deposition is functionalized based on empirical distribution functions in these models. The simplest of these models is uniform gamma energy deposition.

APOLLO2-A takes advantage of the available Method of Characteristics (MOC) solver to calculate the gamma transport for explicit fuel assembly geometry. MOC is known to be accurate for gamma transport just like neutron transport. Section 2.10 of the TR mentions that for industrial applications a simplified gamma source energy smearing across the assembly is performed assuming that gamma energy deposition is flat. The gamma energy depositions in non-fuel regions are also distributed homogenously on fuel pins.

The TR does not include any validation studies for any of the gamma energy deposition models discussed in the TR. Consequently, AREVA was asked to provide details of the smearing model and validation cases for the gamma model intended for licensing purposes. AREVA's response (Reference 2) explained that the gamma energy depositions in fuel pins are calculated by summing all gamma sources and dividing by the number of fuel pins. This simple model is compared to the reference rigorous MOC based model for over 350 validation cases that include simple UO_2, assemblies with gadolinia pins and MOX fuel assemblies. [redacted] This model was replaced by a new simplified gamma transport model. The simplified gamma transport model performs an MOC IDT gamma transport calculation over homogenized pin cells in which fuel, clad and moderator are contained in rectangular meshes. The comparisons of this simplified geometry gamma transport versus the reference detailed MOC transport model show excellent agreement in both pin power distribution and peak pin power.

AREVA also points out that the improvement in the gamma energy distribution calculations does not affect the local uncertainties since the fission density distribution comparisons do not include

gamma calculations. AREVA goes on to state that the calculated global uncertainties are not affected since both ARTEMIS™ and APOLLO2-A gamma energy distributions are calculated by the same model.

AREVA's response indicates that the new gamma model has only been validated against the reference APOLLO2-A gamma model. However, there is no validation of the reference gamma model in the TR. For the MOC based detailed gamma model to be used as a reference, the model should be validated with a range set. Delayed gamma source validation is a particular concern since delayed gammas are responsible for 20 percent of the total gamma source and many Monte Carlo reference codes don't model it. Moreover, as pointed out in the response, the accuracy of the gamma energy deposition model is not accounted for in the local uncertainty calculations. AREVA was asked to provide additional information regarding the gamma model validation.

AREVA provided (Reference 2) a three-step verification to APOLLO2-A gamma model. APOLLO2-A prompt gamma source and gamma transport models are verified by comparing pin powers from prompt gamma against MCNP5 results. For the modeled cases the maximum pin power difference is [redacted] percent.

The values of the delayed gamma energies per fission, used to derive the delayed gamma multipliers to prompt source, are the same in JEFF3.1.1 and ENDF/B-VII for all major fissionable isotopes. Error propagation due to errors in the total gamma source is calculated by perturbing the total gamma source by 10 percent and comparing the pin powers with MCNP5. The peak power error is less than [redacted] percent and considered negligible compared to fission density errors.

The results show that the APOLLO2-A gamma transport model produces accurate results compared to MCNP and the prompt gamma source is implemented correctly in APOLLO2-A. The gamma source sensitivity study shows that the gamma source data uncertainty has negligible effect on the total pin powers. Considering that the delayed gamma energy deposition is a small fraction of the total gamma energy deposition. The gamma source uncertainty also shows that the effects of the delayed gammas are negligible compared to the fission source density errors.

2.6 ARTEMIS™ REFLECTOR TREATMENT

2.6.1 Introduction

The reflector region requires special treatment for 3D simulators. It represents a non-fuel steep flux gradient region made of layers of moderator and stainless steel. One common approach to reflector treatment is to model the effect of the reflector on the core neutronics rather than explicitly modeling the reflector region.

As an example, the albedo model defines a fixed incoming to outgoing neutron current ratio for the reflector. This ratio which is called an albedo can be used in the current nodal solver as a boundary condition. Since the albedo method uses a single value to represent the reflector behavior, it fails to model the effect of the reflector under changing core states. Another common method is to calculate reflector region cross sections using a special 1D problem and using the calculated cross section in a way similar to the fuel nodes in the nodal solver.

2.6.2 Reflector Physics

The ARTEMIS™ reflector model uses a similar 1D problem approach. A 1D fuel assembly, reflector model is solved by APOLLO2-A to provide a heterogeneous response matrix that relates surface fluxes to currents. The same problem is modeled with homogenized regions using diffusion theory. By enforcing the homogenized problem to preserve the APOLLO2-A calculated response matrix, a set of cross sections are calculated for the reflector region. These calculated cross sections are later used in the nodal solver.

The TR states that the ARTEMIS™ reflector model is not necessarily macroscopic and generally the cross sections are transformed [redacted]. However, the TR does not go into detail under which conditions the [redacted] model is used and which model was used for the presented benchmarks. AREVA later clarified (Reference 2) that the reflector model is always [redacted].

The ARTEMIS™ response matrix approach is reported to cause in/out shift of radial powers for heavy (reflectors with a thick steel layer). [redacted]. Because of lack of methodology details regarding [redacted] in the report, AREVA was requested to provide a justification for application of the plant and fuel generic [redacted] cross sections along with a quantification of the magnitude of the [redacted].

AREVA's response (Reference 2) explains that the [redacted]. The average assembly power difference statistics are provided for moderator temperature. Maximum standard deviation in assembly average power density errors are less than [redacted] percent with less than [redacted] percent spread. [redacted], the methodology is robust for PWR applications and acceptable.

2.6.3 Qualification of the ARTEMIS™ Reflector Model

The qualification of the ARTEMIS™ reflector model was performed by comparing ARTEMIS™ generated average nodal powers to 2D MCNP5 reference solution. The validation suite consists of [redacted] cases with boron, moderator density variations for heavy and conventional reflectors and different loading patterns. The maximum deviation assembly average power density is less than [redacted] percent with less than [redacted] percent spread for all cases. The comparison of MCNP5 and ARTEMIS™ results do not show any significant biases with respect to changes in the moderator temperature and boron concentrations. Sample cases were provided by AREVA (Reference 1), showing errors in the power density distributions for a heavy and a conventional reflector models. Based on the 2D assembly power comparisons AREVA concludes that no in/out or azimuthal trends of the error distribution can be identified. However, both power maps in Figures 7.3-4 and 7.3-5 in the TR display clear trends with distance from the reflector. In both reflector types ARTEMIS™ under predicts all peripheral assemblies and over predicts most of the assemblies within 2-4 assemblies from the reflector. In the case of the heavy reflector,

ARTEMIS™ significantly under predicts the power in the center of the core. The contradiction between the results and the statement in the report were brought to AREVA's attention and clarification of the inconsistency was requested.

AREVA stated (Reference 2) in its response that the reflector model is not responsible for the deviations in individual assembly types or local core regions as long as the differences between the power densities in the core center and the periphery are on the same order of magnitude and of the same direction.

AREVA's response required further clarification because it is difficult to distinguish the contribution of the reflector model in assembly power difference oscillations ranging from [redacted] percent to [redacted] percent core wide. It is also not clear why such oscillatory behavior is acceptable as long as the center and periphery assembly power differences are in the same direction as explained in the response. Moreover, for the conventional reflector the MCNP and ARTEMIS™ differences in assembly powers are not in the same direction for the center and the periphery assemblies.

AREVA's response (Reference 2) described the intent of the original statement ("in/out") in greater detail. AREVA understood the staff concerns and the confusion created by the original statement. As a consequence, AREVA provided satisfactory clarification in their response and have suggested via teleconference a better statement for the original TR Section 7.3.2.2.

2.7 ARTEMIS™ VERIFICATION FOR THERMAL-HYDRAULIC MODULE

The stand-alone COBRA-FLX code is implemented as the ARTEMIS™ thermal hydraulic module in ARCADIA®. The stand-alone COBRA-FLX code is documented and reviewed as a separate TR (References 5 and 6). Therefore, the ARTEMIS™ thermal-hydraulic model verification only includes comparisons with the standalone version of COBRA-FLX code for a typical PWR analysis selected at a random state point. The calculated 3D water densities show less than 1.7×10^{-2} percent relative difference with very small standard deviation, which provides some support that the stand-alone version is implemented correctly in the ARCADIA® code system. Ultimately, the NRC staff finds that it is the good agreement between ARCADIA® predictions and measured data from multiple plants and cycles found in the ARCADIA® system validation results (Section 2.9) that demonstrates the stand-alone COBRA-FLX code is implemented correctly in the ARCADIA® system. Because the NRC staff conclusion is based mainly on the ARCADIA® code system validation results, any changes to the COBRA-FLX module will require revalidation of ARCADIA® output using data from multiple plants and cycles.

2.8 VERIFICATION OF THE FUEL ROD MODULE

2.8.1 Introduction

The ARCADIA® Fuel Rod Module results are verified against analytical results for various time dependent power/temperature profiles for uniform fuel rod regions. The validation of FRM relies on the steady state and the transient validation of ARCADIA® code system. Several cases and power profiles such as parabolic and two power distributions in addition to uniform power distributions were validated.

Each verification case aimed to test different capabilities of the FRM. For all cases outer most and the inner most temperature difference was found to be below 1 percent with less than

1.5 percent error in the outer heat flux. The results show that the numerical solutions are consistent with the known analytical solutions.

2.9 ARCADIA® BENCHMARKING RESULTS

2.9.1 Validation

An extensive validation suite is presented for ARCADIA® validation in the TR. 1D axial and 2D radial core nodal powers, rod and boron worths were compared to the measured values for 6 different PWR reactor types with 6 different fuel types for a total of 52 cycles of operation. The summary of the benchmark cases is given in Table 3.

Table 3: ARCADIA® Benchmark Suite

Vendor	No. Fuel Assemblies	Fuel Type	Plants	Number of Fuel Cycles	Enrichment Range	Gd_2O_3 Enrichment
Westinghouse	157	17x17	A, B, V1	14 + 1 + 5	1.8-4.95	2-10
Westinghouse	193	17x17	S1 + S2	3 + 3	4.2-4.8	2-8
CE	217	14x14	C	9	2.7-4.50	2-8
Siemens	177	15x15	G1	5	3.5-4.4	2,5
Siemens	193	18x18	G2	5	1.9-3.45	5,7
B&W	177	15x15	T1	7	2.85-4.9	2, 3, 8

ARCADIA® benchmark results are evaluated for startup physics test measurements and core follow measurements.

2.9.2 Startup Physics Test Measurement

For each of the cycles shown in Table 2, the calculated critical boron concentration, individual control rod worths, total control rod worth and isothermal temperature coefficients are compared to the measured values for beginning of cycle (BOC). The acceptance criteria for the benchmarks were adopted from American Nuclear Society (ANS standards), References 8 and 9.

The TR states that the measured data for startup physics was adjusted to reflect ARCADIA® delayed neutron parameters for comparisons. However, neither calculation of the adjustment parameters nor the details regarding quantification and justification of adjustment of the measured data were provided. In order to assess the accuracy of ARCADIA® results, details of the mentioned adjustment was requested from AREVA.

AREVA's response (Reference 2) explains that the set of kinetic parameters used in the plant computer to calculate reactivity are different than the ARCADIA® calculated kinetic parameters. Therefore, β_{eff} for the measured data was adjusted to be consistent with the ARCADIA® β_{eff}. AREVA's response also includes sample adjustment data for four different plants to show that the adjustment can be as large as 4 percent for some cycles; however it is around 2 percent for most cycles. Considering that the adjusted value can change based on the raw data and the

methodology used in calculation, such adjustment is necessary for consistent comparison of the predicted and measured values.

As part of the startup physics validation, the measured rod worths are compared with the ARCADIA® predicted values in this section. Different rod worth measurement techniques are practiced in the industry today. Due to this variation, the provided measurement data from different plants and cycles can be expected to have similar variations in the measurement accuracy. For example, a rod worth calculated by rod swap technique can be more accurate than the one calculated with boron swap technique. During the review, the NRC staff was concerned that the ARCADIA® methodology can present different biases and trends compared to different measurement techniques. Therefore, AREVA was asked to provide the rod worth measurement technique with each set of results, and to provide a conclusion about the accuracy of the method vs. each technique.

AREVA provided a table (Reference 2) showing which measurement method was used in each cycle of each plant along with additional information regarding the advantages and accuracy of each technique. Only rod and boron swap methods were used in all benchmark cases and as expected, ARTEMIS™ results are more consistent with the rod swap measurements. However, ARTEMIS™ methodology shows good agreement with both techniques and all benchmark cases deemed acceptable.

2.9.2.1 Startup Physics Summary for Plant A, Cycles 1-14

The BOC HZP ARCADIA® predicted critical boron concentrations were compared to the measured critical boron concentrations for 14 cycles of Plant A. The ARTEMIS™ results meet the 50 ppm acceptance criterion (Reference 9) for 12 cycles. In the remaining 2 cycles the predicted critical boron concentration is different than the measured value more than 50 ppm. Therefore, the second less conservative 500 pcm equivalent boron worth criterion is selected for the failed cases. In order to be able to use the second criteria the difference in boron concentrations should be converted to reactivity equivalent using boron worths. The TR doesn't specify how boron worths are calculated for the two failed cases. The TR also doesn't mention any B^{10} adjustment for the calculated boron worths. Since the neutron absorption by boron is mainly due to B^{10} isotope, the B^{10} concentration in the borated water can change with depletion as well as insertion of fresh borated water into the system. Thus, variation in the B^{10} concentration should be accounted for in boron worth calculations.

AREVA was asked to provide information regarding calculated or measured boron worth used for reactivity comparisons. If the calculated boron worth was used, a justification was requested using the calculated boron worth when the error in the calculated boron concentration exceeds the boron concentration criteria. AREVA was also asked if the boron worth used in the reactivity calculation was adjusted for the B^{10} isotopic abundance.

AREVA responded (Reference 2) by explaining that since no measured boron worth data were available for the mentioned two cycles, respective predicted boron worths were used to calculate the reactivity equivalent of the boron concentration differences. As justification of this approach, the available measured to calculated boron worth comparisons for 5 cycles of plant A and a total of 6 cycles of S1 and S2 plants were also provided. The difference between calculated and measured (C-M) boron worth changes between -0.27 and +0.35 pcm/ppm for the presented benchmark cases. Even when the maximum boron worth under prediction (-0.27 pcm/ppm) is used as boron worth bias, the critical boron concentration difference for all

benchmark cases stays below 500 pcm. Therefore AREVA's methodology to apply the 500 pcm acceptance criteria for the two mentioned cycles is acceptable

AREVA also confirmed that the measured boron concentrations were adjusted for B^{10} content to match 19.9 percent ARTEMIS™ internal value for a consistent comparison. When the ARCADIA® boron worth predictions are compared to adjusted Plant A measurements, and to unadjusted plant S1 and S2 measurements, the improvement in the results was apparent. In addition, even for the cases with no adjustment the ARCADIA® predictions showed good agreement with the measurements.

As part of the startup physics validation, when the predicted and measured control rod worths are compared, the ARCADIA® predictions for all individual rod banks except bank D passes the 15 percent acceptance criteria for all 14 cycles at BOC HZP (Hot Zero Power) conditions. Bank D control rod worth relative difference between the measured and the predicted values in cycle 11 is 15.1 percent. AREVA considers the bank D rod worth measurement in cycle 11 as an anomaly, since the bank D worth predictions are all acceptable under the acceptance criteria for the previous and later cycles. However, this explanation isn't considered satisfactory and AREVA was asked to provide further justification for bank D data to be excluded from the benchmark results, since without a detailed analysis of other cycle differences (core design, flow condition, rod shadow, etc.), benchmark data shouldn't be excluded from the suite.

AREVA's response to the RAI (Reference 2) explains that the text in the report is misleading. The failure of Bank D prediction is in the acceptable failure rate of 0.4 percent and therefore, ARCADIA® is not considered as failed in rod worth measurements. However, bank D worth is included in the total control rod worth calculation. Even though ARCADIA® predicts the bank D rod worth with an error 0.1 percent more than acceptance criteria, when all plant data is considered, 95/95 tolerance limit for single bank worths results in less than 15 percent uncertainty.

2.9.2.2 Startup Physics Summary for Plant B Cycle 1 and Plant C, Cycles 10-18 and Plant G1 Cycles 26-30

Additional Startup Physics Summary for Plant B Cycle 1, Plant C Cycles 10-18 and Plant G1 Cycles 26-30, were reviewed and found to be acceptable. However, ARCADIA® calculated critical boron concentrations results fail to meet 50 ppm criterion for three out of five cycles of Plant G1. Therefore, the acceptance criterion is switched from 50 ppm to 500 pcm equivalent boron concentrations for the three cycles. The cycles failed for the 50 ppm criterion are shown in Table 4.

Table 4: Plant G1 Failed Cycles

Cycle	C-M Critical Boron Concentration	500 pcm Equivalent (C-M)Boron Concentration
28	-58	-60
29	-55	-61
30	-58	-63

Cycles 27 and 28 had a BOC B^{10} abundance of 19.2 percent. Whereas Cycles 29 and 30 contained about 30 percent enriched boron. The ARCADIA® TR states that Cycle 26 measured value may be suspect because the B^{10} abundance was not measured. Since the B^{10}

abundance didn't change in Cycles 27 and 28 the same value was assumed for Cycle 26. However, considering that there are no unexpected results for Cycle 26 HFP comparisons, no additional B^{10} correction should be necessary at HFP. AREVA was requested to provide justification for the statement about Cycle 26 measurements and additional information since the TR does not clearly describe which boron measurements are adjusted for B^{10} content, and which are not. B^{10} corrections, both at HZP and HFP (i.e., B^{10} depletion, if included) should be applied consistently for all cycles and should be clearly documented.

AREVA's response (Reference 2) pointed out an error in the reported results. Since the B^{10} abundance didn't change in Cycles 27 and 28 the same 19.2 percent abundance is assumed for cycle 26. However, erroneously, the B^{10} adjustment was made to the ARCADIA® calculated values instead of the measured critical boron concentrations using the measured or the assumed (for Cycle 26) B^{10} abundances. Additionally, the measured values were adjusted to 19.74 a/o B^{10} instead of the 19.9 a/o B^{10} abundance internal to ARTEMIS™. Therefore, the results presented in Table 28-G1-1, Table 28-G2-1, Figures 28-G1-1 through 28-G1-5 and Figures 28-G2-1 through 28-G2-5 are stated as erroneous and the new set of tables and figures are provided in the response. Based on the corrected results the critical boron (C-M) values are shown in Table 5.

Table 5: Plant G1 Originally Failed Cycles

Cycle	C-M Critical Boron Concentration
28	-45
29	-41
30	-44

2.9.2.3 Additional Startup Physics Summary

Additional Startup Physics Summary for the remaining plants presented in the TR were reviewed and found acceptable.

2.9.3 Core Follow Measurements

Benchmark results from 52 cycles of 9 plants are presented. For each cycle, critical boron concentration, assembly average power distribution and core average axial power distribution predictions are compared to the measured plant data. Boron concentrations are compared at each measurement point whereas power comparisons are performed at least at BOC, MOC and EOC. The acceptance criterion is selected as less than 5 percent RMS for power comparisons.

The TR presents boron letdown curves for each cycle individually as a function of fractional cycle length. This scale prevents any cycle to cycle comparisons and inhibits the ability to approximate cycle length-based effects, such as gadolinia depletion, B^{10} depletion, and design implications for 24 vs. 12 month cycles. Furthermore, the letdown curves are presented on an absolute value scale, which makes individual deviations very hard to discern. The NRC staff requested AREVA to provide a better scaling for the boron letdown curves and a cumulative critical boron concentration differences plot for all cycles of each plant for cycle to cycle comparisons.

In response, (Reference 2) AREVA provided a new set of plots for boron letdown curves. (C-M) boron concentrations are plotted as a function of cycle burnup for all cycles on a single plot for each plant. No obvious bias or trends are observed in ARTEMIS™ critical boron concentration predictions for core follows.
As expected the measured average axial power shapes have the similar axial power shape in all plants. A representative profile is shown in Figure 1. The grid spacer effects (grid depressions) seen on Figure 1, is common in axial power profiles of all plants except plant C and plant T. The plants C and T exhibit axial power shapes similar to the profile depicted in Figure 2. The smooth axial shape suggests that the power profile plots are not obtained from the actual detector readings but from reconstructed power shapes detector readings. However, the TR does not provide any information regarding the detector type or the power reconstruction method used in plant benchmarks. Consequently, AREVA was asked to provide further details for plant data and the interpolation/extrapolation method used to reconstruct the axial power shape if fixed core detectors were used in any plants.

AREVA provided (Reference 2) a table showing the detector type used in each plant in response to the RAI. As predicted, fixed incore Rhodium detectors are used in plants C and T. After detector power coefficients are calculated, detector inferred powers are linearly interpolated for each 24 axial node for comparison with the ARTEMIS™ predicted power. Based on the ARCADIA® benchmark results, this simple approach produces satisfactory results.

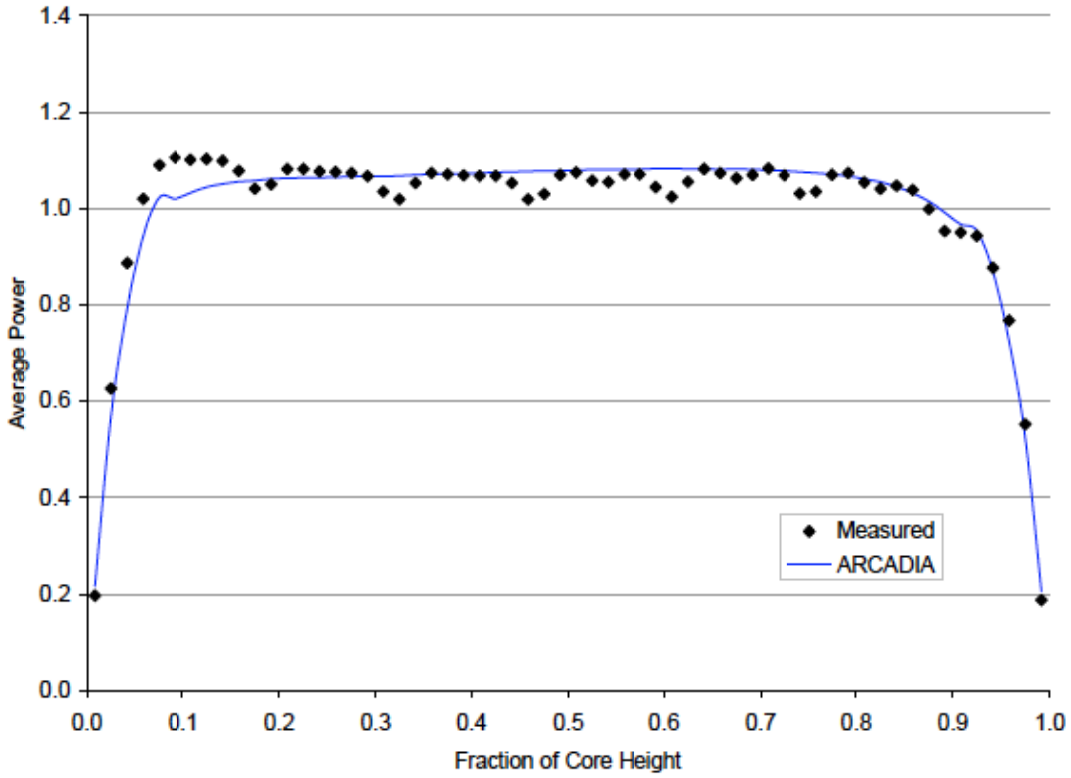

Figure 1: Representative Axial Power Shape with Grid Depressions

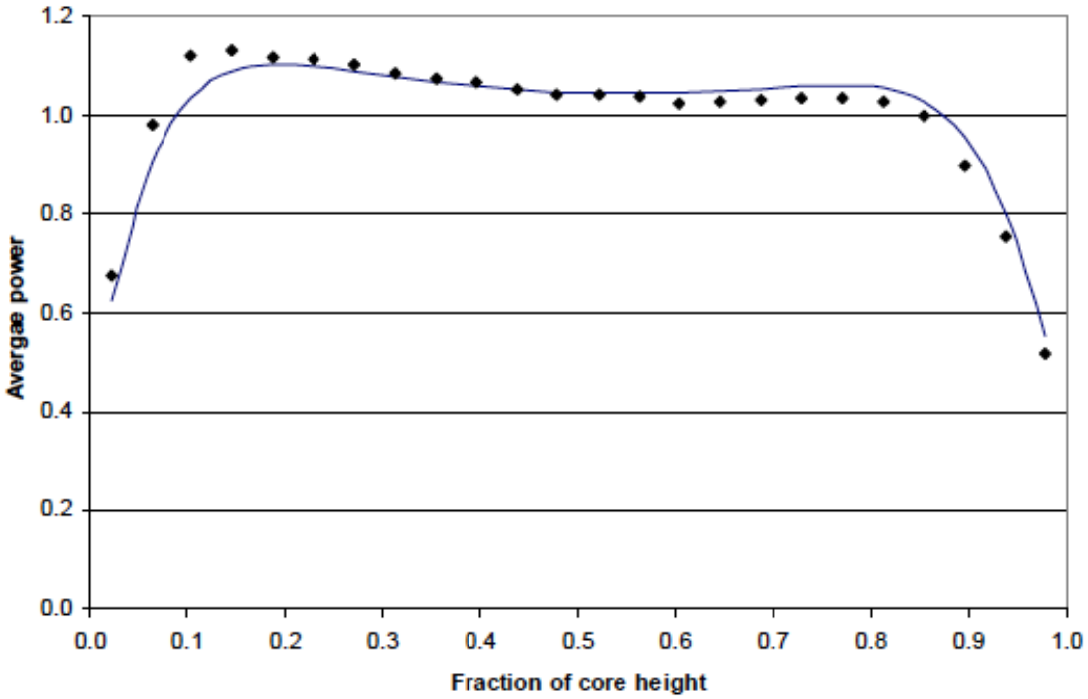

Figure 2: Representatives Axial Power Shape Profile for Plants C and T

In general, when ARTEMIS™ core follow benchmark results are reviewed, small trends with respect to Gd_2O_3, U_{235} enrichments and fuel types can be seen in some cycles. However, no significant or unusual biases or trends in critical boron, assembly power and core average axial power distribution predictions were observed.

Additional results were presented in the TR for a number of plants. All presented results meet acceptance criteria.

Except for Plant G2 cycle 1, all presented results meet acceptance criteria. The Plant G2 Cycle 1 BOC axial power distribution exceeds the 5 percent criterion. The RMS value of the measured and predicted power difference is 6.5 percent for Plant G2 cycle 1 at BOC. Measured powers can also be as different as 20 percent at some axial locations. Considering that plant designated as G2 was operated in a "load follow mode" in the first cycle, indicating that the reactor core was not operated at steady state, a steady state mode core simulator can be expected to produce less accurate results than the regular time dependent operation. For all other cycles ARTEMIS™ axial RMS results are below 4.4 percent.

2.10 VALIDATION OF ARCADIA® TO TRANSIENT BENCHMARKS

2.10.1 ARTEMIS™ Comparison to TWIGL-2D Benchmarks

In this section, the ARCADIA® code system is benchmarked against established benchmark problems without thermal feedback. The benchmarks selected are the TWIGLE-2D step transient and the TWIGL-2D ramp transient analytical solutions.

Comparisons of ARTEMIS™ are made against the established benchmark. The TWIGL Seed-Blanket problem consists of a square array reactor, which contains three compositions. A single delayed group is used and the problem involves only a neutronics calculation (with no transient moderator or fuel temperature effects). The simulation of ARTEMIS™ for these benchmark problems is possible because the mesh in the reference solution is sufficiently fine to qualify as a reference solution. Two cases were to compare to the TWIGL-2D benchmark, a step change in reactivity and a ramp change in reactivity.

The TWIGL-2D step transient, typical of a rod ejection event, involved an immediate reduction in the thermal absorption cross-section for one composition fuel type at the beginning of the transient.

The TWIGL-2D ramp transient, typical of a control rod withdrawal, involves the same cross-section change as in the step transient except the change occurs linearly from 0.0 to 0.2 seconds.

AREVA provided results of the comparisons in the form of figures and tables. Both the step transient and the ramp transient indicate excellent agreement between ARTEMIS™ and the respective benchmarks (Figures 11.1-1 and 11.1-2) of Reference 1. The excellent agreement is indicative of the correct formulation of the neutronic equations in ARTEMIS™.

In addition to the comparison of ARTEMIS™ to the TWIGL-2D benchmarks, ARTEMIS™ was also compared to Nuclear Energy Agency Committee on Reactor Physics (NEACRP) benchmarks.

2.10.2 ARTEMIS™ Comparison to NEACRP Benchmarks

The NEACRP benchmarks are a set of analytical benchmarks. The specification document for these benchmarks is found in Reference 11.4-1 of the submittal, Reference 1. This reference defines the core configurations, inputs, and conditions to be used for each transient modeled with ARTEMIS™. The core modeled in the PWR transient, is a 157 fuel assembly core. The nuclear data and its dependence on boron, moderator density, moderator temperature, fuel temperature, and control rods are defined in the reference. The reference also defines clad and fuel thermal properties.

Six cases (A1, A2, B1, B2, C1, and C2) were considered in the NEACRP benchmark problem. The cases considered represented control rod ejections from three different configurations (A, B, and C) and from both zero power (1) and full power (2) conditions.

In the Case A transients, the center rod is ejected. In the Case B transients, a set of four periphery rods are ejected. Finally, the Case C transients eject a single periphery rod in the core. The zero power cases eject a fully inserted control rod and the full power cases eject a partially inserted control rod. The NEACRP cases provide a range of reactivity insertions and core conditions that provide an effective test of the coupled neutronics, fuel rod, and thermal-hydraulics transient responses by the ARTEMIS™ code system.

A summary showing the results for several industry codes used to model the NEACRP control rod ejections were compiled (Reference 10). The results from the PANTHER code (Reference 11) are typically used as the reference solution for the NEACRP control rod ejection benchmark cases. The reference results are included for comparison to ARTEMIS™.

Comparisons of important steady-state parameters between ARTEMIS™ and the reference case are provided in Table 11.2.2-1 of Reference 1. These conditions define the starting point prior to the transient. Agreement between the two codes is excellent. Boron concentrations are within 9 ppm. Full power effective Doppler fuel temperatures are within 2.5°C. The initial local peak is within 0.6 percent. The reactivity release for each case is within 4 percent. The reactivity release is the worth of the ejected rod with feedbacks on at the initial power level. The steady state comparisons verify that the input data is correct and that the static calculations using that data are very similar. Therefore, the initialization of the two codes, the reference code, PANTHER, and ARTEMIS™ are equivalent. Detailed comparison results are provided in Reference 1.

In general, the results show that the ARTEMIS™ code with the time dependent solutions neutronics coupled with the time dependent solutions for the fuel temperature and coolant properties, appropriately model the time dependent phenomena.

2.11 POWER DISTRIBUTION UNCERTAINTIES

2.11.1 Introduction

During a reactor operation, assembly peaking factors are checked at certain intervals to operate under licensed limits. The two peaking factors, enthalpy rise hot channel factor ($F_{\Delta h}$) and heat flux hot channel factor (F_Q) refer to relative maximum fuel rod linear power and relative maximum fuel rod heat flux. For practical purposes, $F_{\Delta h}$ and F_Q can be interpreted as the pin peaking factor and pellet peaking factor, respectively. These peaking factors are calculated by two methods during the reactor operation.

Detector responses: Nodal powers converted from the measured detector powers using the core simulator, for the available detector locations. For other locations without a detector reading, the detector responses are “inferred” using the core simulator and detector response reconstruction algorithms implemented in the core monitor. Later, the nodal powers are converted to pin powers using the core simulator.

Simulator predictions: Pin powers are directly calculated from the predicted nodal powers using the core simulator.

In order to operate under licenses limits for the peaking factors, the application uncertainties associated with inferred and calculation uncertainties (Nuclear Reliability Factors) should be well established. The common contributors to the uncertainty in both methods are pin (local) and assembly (global) power predictions by the core simulator.

The TR first establishes local peaking factor uncertainties then calculates inferred uncertainties based on plant type and finally provides limits for the Nuclear Reliability Factors (NRF).

2.11.2 Local Peaking Uncertainty

The uncertainty in ARTEMIS™ pin-power predictions can be split into two main components:

a) Uncertainty in fuel assembly pin powers due to uncertainties in the methodologies implemented in APOLLO2-A and uncertainties in the nuclear data used in calculations.

b) Uncertainty due to ARTEMIS^{TM} pin power reconstruction methodology, itself, and the uncertainty in the data due to reflective boundary condition assumption used in APOLLO2-A lattice calculations.

The accuracy of APOLLO2-A predicted fission density distribution for the critical experiments is shown in APOLLO2-A validation section of the TR. In order to establish pin power uncertainties in APOLLO2-A calculations, AREVA selected 6 B&W 1980 critical experiments representing 15x15 and 16x16 fuel assemblies, out of 22 critical experiments presented in APOLLO2-A validation. The TR states that this subset of critical experiments was selected since they are the most recent experiments with low measurement uncertainties. However, the TR does not mention elimination of 14x14 and 17x17 lattices that existed in the B&W 1980 criticals. The RMS values of B&W 1980 criticals are also smaller in comparison to the other criticals in the validation suit. Moreover, the B&W 1980 criticals that were used in APOLLO2-A validation do not include the mentioned 16x16 lattice cell configuration. AREVA was requested to provide further justification for selection of the critical experiments to be used in uncertainty analyses, as well as the inconsistency in the lattice cell configurations used in APOLLO2-A validation and APOLLO2-A pin power uncertainty calculations.

AREVA's response (Reference 2) explains that the critical experiment data used in the local uncertainty analysis of APOLLO2-A was selected based on the licensing studies of the previous code systems for consistency (References 9, 12, and 13). However, AREVA also provided the following justification for the selected subset of B&W 1980 criticals:

i) The standard deviations of B&W 1980 criticals are representative of criticals with PWR like core configurations. The lattices were designed after realistic 15x15 and 16x16 PWR lattice configurations.

ii) B&W 1980 critical experiments are the only experiments that provide complete central zone measurements.

iii) B&W 1980 experiments are one of the relatively newer experiments and they have lower measurement uncertainties.

iv) The standard deviations calculated from B&W 1980 criticals only include the central zone assembly data.

AREVA's response is satisfactory. APOLLO2-A models fuel lattices using reflective boundary condition. In order to assess the APOLLO2-A pin power uncertainties separately from multi-assembly de-homogenization, a bundle with close to zero radial leakage should be used for consistent comparison. When the criticals with void fractions, incomplete fission density distributions and non-practical configurations are eliminated, B&W 1980 criticals remains as the best set of criticals from the available data.

AREVA also clarified that the inconsistency in the B&W lattice types mentioned in APOLLO2-A validation and the uncertainty analyses originates from a typographical error. The APOLLO2-A validation suite indeed includes 16x16 lattice configurations.

The relative pin power errors for B&W 1980 core 1 criticals show that the standard deviation is below 0.8 for all criticals. Based on the different gadolinia loadings and enrichments used in the selected criticals, the calculated uncertainty is representative of pin power uncertainty for

lattices with 1.94 percent to 4.02 percent U^{235} enrichment and up to 4.0 percent Gd enrichments.

The TR states that no biases are observed regarding modeling of water holes or poisons; however, in most of the critical core configurations (cores 4, 5, 12, 14, 18) the fuel rod next to the instrument tube has a much higher error than most of the other fuel rods. Also the gadolinia fuel pins in cores 5, 14 and 20 clearly demonstrate a substantial bias (up to [redacted] percent deviation) as compared to non-gadolinia fuel rods. AREVA was requested to comment on this contradicting observation to the statement in the TR.

AREVA's stated in their response (Reference 2) that, "No biases are observed around water holes or poisons" is, in hindsight, misleading. What was intended to be stated in the TR was that, relative to the previous code systems, the strong biases seen with previous code systems are no longer seen with APOLLO2-A.

AREVA also confirms the bias in gadolinia pin power predictions and the bias in fuel pin power predictions next to instrument tubes. The source of the bias around the instrument tubes is partially attributed to missing detector model in APOLLO2-A for the instrumented cores. When the detectors are modeled, the biases in most cores decrease.

Possible sources of gadolinia pin biases are also discussed in detail in the AREVA's response. The effects of physical properties of gadolinia pins, gadolinia density and fast to thermal fission ratios on gamma ray emission are debated. As a conclusion, the bias in gadolinia pin power comparisons are attributed to the measurement errors in the low powered gadolinia pins. AREVA's analyses for the observed biases are determined to be reasonable.

The TR also notes that local peaking uncertainty analyses exclude fuel pins with relative power less than [redacted]. The non- gadolinia pin power standard deviations in cores with gadolinia are approximately the same as the experiments without gadolinia. The application range in the report states that the comparisons included "Gadolinium poison up to 10 weight percent in UO_2 fuel." Nevertheless, the TR does not include the uncertainty in fuel rods with gadolinia (which is calculated with up to 6 percent). Justification for the specified application range was requested from AREVA.

In their response (Reference 2), AREVA argues that when gadolinia is present in the gadolinia pins, the uncertainty is higher. However, gadolinia pins are at low power and never limiting. However, when the gadolinia in a gadolinia pin is depleted the uncertainty statistics are equivalent to pin power uncertainties in non-Gd fuel assemblies. Therefore, the claimed application range is valid. AREVA's point of view is reasonable and AREVA's response is acceptable.

The second contributor of the local peaking uncertainty can be calculated from multi-assembly (color set) calculations. In these calculations, pin powers in multi bundle configurations (2x2) with different enrichments and poison contents are calculated using the lattice physics code (APOLLO2-A) and considered as the reference solution. Then the reference solution is compared with the pin powers calculated by the core simulator (ARTEMIS™) using the homogenized lattice data and form factors provided by the lattice physics code from the solution of the individual lattice calculations.

The TR provides statistics from pin power comparisons of 22 multi-assembly calculations. The U^{235} enrichments range from 2.25 percent to 4.95 percent in the modeled sets. 20 of these sets include gadolinia pins with enrichments ranging from 2 percent to 10 percent. 40 GWd/mtU and 20 GWd/mtU depleted lattices are also used in the lattice combinations. Each color set was depleted around 20 GWd/mtU to cover a range of depletions 0 GWd/mtU to 60 GWd/mtU for each pin power comparison. Two of the sets depleted with rodded assemblies.

The results show that the maximum relative error in peak pin powers is [redacted] percent. The relative pin power RMS error is less than [redacted] percent with a standard deviation of [redacted] percent. The maximum relative pin power error is [redacted] percent for a gadolinia pin next to a rodded fuel lattice. A combination of gadolinia depletion errors and relatively larger flux gradient at the periphery to a low power fuel assembly can lead to large errors in the predicted pin powers. Considering that a gadolinia pin is not expected to be the limiting pin and control rods are not fully inserted during normal PWR operations, this large error is considered as an outlier and ignored. AREVA takes a conservative approach in calculation of the de-homogenization errors and considers the statistics from only the pins around the periphery that have relatively higher mean and standard deviation, [redacted] percent and [redacted] percent, respectively.

The multi-assembly calculations cover a wide range of burnable poison and fuel enrichments for an acceptable depletion range. Since not all lattice physics codes are capable of handling multi bundle configurations, de-homogenization and boundary condition errors are often not accounted in uncertainty calculations. Based on the different configurations modeled in multi-assembly calculations, the calculated de-homogenization uncertainty can be considered as representative of typical PWR simulations.

2.11.3 Inferred Power Distribution Uncertainty Analyses

The inferred power distribution uncertainty refers to the power distribution prediction uncertainty at missing detector locations. A missing detector location can be a fuel bundle without a detector or a fuel segment located between two fixed incore detector locations. For both types of inferred uncertainties the methodology is similar. First a power map (radial or axial) is obtained from all the available detector locations, then a detector reading at a radial or axial position (in one of the fixed core detectors) is assumed not to exist and the missing measurement is reconstructed using a reconstruction methodology which involves simulator calculated values. The difference between the measured and inferred ($F_{\Delta h}, F_Q$) values are noted as the global component of the inferred uncertainty for each hot channel factor. Finally, the local peaking and de-homogenization uncertainties are added to the global uncertainties to calculate the total inferred uncertainty.

ARCADIA® uncertainty analyses presented in the topical report are similar to the described methodology. The inferred uncertainties are calculated for three different incore measurement systems used in current PWR reactors. The inferred global uncertainty is combined with local peaking and de-homogenization uncertainties to calculate normal uncertainty and non-parametric uncertainty using Monte Carlo method. Conservatively, the maximum of the two uncertainties is selected as the inferred uncertainty. Since the inferred uncertainties include local and global uncertainties, the total inferred uncertainty is comparable to measurement uncertainties. Therefore, acceptance criteria for the inferred uncertainties are based on the measurement system uncertainties reported in previously licenses methodologies (References 14, 15, and 16).

Three measurement systems, INPAX-W, INPAX-CE and MEDIAN AMS, are evaluated for the inferred power distribution uncertainties. Since the uncertainty analysis only includes these specific measurement systems, AREVA was asked to restrict the ARCADIA® application range to the mentioned measurement systems.

In their response, AREVA proposed (Reference 2) the following sentence to be included in Section 13.1 of the TR:

> "These benchmarks include uncertainty verification for plants that use moveable incore, Rh fixed incore, and Aeroball incore detectors. AREVA will continue to monitor its methods with respect to current cycle designs for its licensing applications. Prior to licensing a new contract, AREVA will evaluate at least three cycles of data relative to these criteria prior to licensing the first cycle with AREVA fuel with ARCADIA®. This includes verification of their measurement uncertainties and/or calculation uncertainties by using the appropriate method presented in Section 12 of the TR (Reference 1)."

2.11.3.1 INPAX-W Reconstruction Methodology

This measurement system is used in Westinghouse plants. 15 cycles from 4 plants are used for INPAX-W inferred uncertainty analyses. $F_{\Delta h}$ and F_Q uncertainties are calculated as [redacted] and [redacted], respectively. These uncertainties are less than the acceptance criteria and acceptable.

2.11.3.3 INPAX-CE Reconstruction Methodology

The INPAX-CE system is designed for Combustion Engineering plants. INPAX-CE system consists of fixed core detectors. The missing axial detector location in the INPAX-CE system introduces additional uncertainties compared to INPAX-W systems. The reconstruction uncertainties for assembly power to average detector power and peak planar power to assembly power are calculated using INPAX-W systems. Since fine motion detector readings are available in an INPAX-W system, using the inferred power uncertainty methodology described earlier, the detector powers are aggregated to the fixed detector locations and inferred detector powers are calculated for the missing detector axial locations. Although the inferred uncertainties are calculated for INPAX-W system, the uncertainty associated with the reconstruction algorithm is independent of the system therefore it is applicable. 13 cycles from 3 plants are analyzed for INPAX-CE reconstruction uncertainties. $F_{\Delta h}$ and F_Q uncertainties are calculated as [redacted] and [redacted], respectively. These uncertainties are less than the acceptance criteria and are thus, acceptable.

2.11.3.4 MEDIAN AMS Reconstruction Methodology

The Measured Dependent Interpolation Algorithm Using NEM (MEDIAN) Aeroball Measurement System (AMS) is the measurement system used in the German reactors and planned to be used in the United States Evolutionary Power Reactors (USEPR) plants. 10 cycles from two plants are used for uncertainty calculations. The standard deviation of the inferred uncertainties for $F_{\Delta H}$ and F_Q are [redacted] percent and [redacted] percent, respectively. The standard deviations of the total uncertainty including the local uncertainties are [redacted] percent and [redacted] percent, respectively. Both uncertainties are below the selected criteria of 4.1 percent for $F_{\Delta H}$ and 5.1 percent for F_Q and thus, acceptable.

2.11.3.4 Calculated Power Distribution Uncertainty Analysis (Nuclear Reliability Factors)

The Nuclear Reliability Factors (NRF) for $F_{\Delta H}$ and F_Q are determined similar to the inferred uncertainties described in the previous section. The difference between the two uncertainties is that the global component of the inferred uncertainty is a measure of how well the instrument readings at un-instrumented locations are predicted, whereas in the NRF, it is a measure of how well the simulator can predict the assembly power at instrumented locations. In the ARCADIA® methodology, after global uncertainties are calculated by comparing the detector measured versus the simulator-calculated powers, the local peaking uncertainties are combined to calculate normal and non-parametric uncertainties. The more conservative of the two uncertainties are selected as the bounding uncertainty. The acceptance criteria for the NRFs are selected from the previously accepted values (Reference 14) as 3.8 percent and 4.8 percent for $F_{\Delta H}$ and $F_{Q,}$ respectively.

40 cycles from 9 plants are selected for uncertainty analysis. These plants and the cycles also include the plants and cycles used in all three inferred uncertainty analysis. Corollary, the NRF analysis includes all PWR plant types mentioned in the TR. The global uncertainty standard deviation is [redacted] percent for [redacted] data points. When local uncertainties are combined with the global uncertainties, the standard deviation for $F_{\Delta H}$ and $F_{Q,}$ are calculated as [redacted] percent and [redacted] percent, respectively. Since both uncertainties are below the acceptance criteria, ARCADIA® NRFs are acceptable.

The TR states that plant G1 has a 2 percent bias for the peak assemble power comparison associated with grid depressions. However, analysis of the average axial power plots for G1 indicates this deviation is possibly due to an increased difference in core average axial offset and not the lack of compensation of an explicit grid flux. AREVA was requested to comment on this statement.

In their response, AREVA explained (Reference 2) that even although the statement was included in the paragraph that discusses grid depression effects, it was not intended to attribute the 2 percent bias to grid depression but simply to explain the procedure if such a bias was observed in a axial power profile. AREVA states that plant G1 doesn't use the uncertainty approach mentioned in this section but if it did, such a large bias would need to be resolved. AREVA also agrees that from the average axial profile it seems like a bias is caused by an inaccurate prediction in the axial offset. Considering that plant G1 doesn't use this uncertainty approach AREVA's explanation is satisfactory.

Plant B and Plant G2 have Inconel grids in cycles 1 and 2. Since Inconel grids cause large grid depressions and are no longer used, these data are not included in the peak uncertainty analysis. Therefore, AREVA was asked to limit ARCADIA®'s application range to non-Inconel grids.

AREVA stated in their response that (Reference 2) the exclusion of Inconel grids does not impact the qualification of ARCADIA®. However, the NRC staff contends that peak prediction uncertainties need to be addressed for each grid type and plant. As such, AREVA proposes to add the following sentence to the TR:

"During the verification of uncertainties, any peaking biases due to grid type or other plant effects will be quantified and accounted for in the uncertainties and/or peaking allowances in the licensing calculations on plant specific basis."

2.12 SUMMARY AND QUALIFICATION METHOD

2.12.1 Range of Applicability

The intended application range for ARCADIA® code system is explained in this section. However, the intended application range for the PWR lattices is not clear as stated in the TR of Reference 1. Consequently, AREVA was asked to clarify if the intention to license the ARCADIA® code system for only the benchmarked lattice geometries, as stated in the TR of Reference 1, or any PWR lattice geometry with 4 cell water holes or less. If an approval for general pin lattice geometry is requested, a justification for the generalized application range is requested.

AREVA responded to the NRC staff's concern (Reference 2) by pointing out that based on the benchmark results no clear trends or biases are observed with different lattice geometries. The NRC staff did not agree with this position and stated that the ARCADIA® code system accuracy does depend on the lattice geometry and that a licensing approval will be required for a general PWR lattice geometry. AREVA also pointed out that AREVA has committed to evaluate at least three cycles of existing plants data against the criteria in Table 13.2-1 of the TR, prior to applying ARCADIA®.

AREVA's response was not found to be satisfactory, as no benchmark or uncertainty analysis is provided in the TR for lattices with IFBA fuel rods. IFBA geometry is challenging for lattice physics code and pin power uncertainties may not be bounding for IFBA pins.

Consequently, AREVA provided a second response to the RAI via teleconference. In the second response, AREVA presented comparisons of APOLLO2-A and MCNP calculated eigenvalue and fission density distributions for a PWR lattice with IFBA fuel pins. The eigenvalue differences are less than [redacted] pcm with less than [redacted] percent RMS in fission density distributions and less than [redacted] percent difference in peak pin values for three different state points. The results show that APOLLO2-A can accurately model IFBA type fuel pins and applicability of ARCADIA® code system to IFBA fuel types is acceptable.

3.0 LIMITATIONS AND CONDITIONS

Based on the technical evaluation above, the NRC staff finds the ARCADIA® code system methodology for PWRs acceptable for licensing applications, subject to the following limitations and conditions:

1) The range applicability of the ARCADIA® code system Methodology is restricted to the fuel data provided in the TR, unless additional analysis and benchmarking is conducted to validate the ARCADIA® code system to a fuel type not mentioned in the TR (Reference 1).

2) The benchmarks provided in the TR (Reference 1) include uncertainty verification for plants that use moveable incore, Rh fixed incore, and Aeroball incore detectors. AREVA will continue to monitor its methods with respect to current cycle designs for its licensing

applications. Prior to licensing a new contract, AREVA will evaluate at least three cycles of data relative to these criteria prior to licensing the first cycle with AREVA fuel with ARCADIA®. In addition, application of the ARCADIA® code system to a new uncertainty measurement system(s) would require review and approval by the NRC staff prior to implementation. This includes verification of their measurement uncertainties and/or calculation uncertainties by using the appropriate method presented in Section 12 of the TR.

3) The ARCADIA® code system is limited to fuel types with non-Inconel grids unless additional verification of uncertainties is conducted to account for any peaking biases due to grid type or other plant effects. Verification of uncertainties must be quantified and accounted for in the uncertainties and/or peaking allowances in the licensing calculations on plant specific basis.

4) For any changes made to the stand-alone version of COBRA-FLX that is implemented in the ARCADIA® code system (the COBRA-FLX module), AREVA will revalidate the ARCADIA® code system output using measured data from multiple plants and cycles.

4.0 CONCLUSION

The technical review of application methodology and benchmarking results of the ARCADIA® code system for application to neutronic design analyses of pressurized water reactors (Reference 1) has been completed. The documentation provided in the TR and the responses to the RAIs demonstrate that the analytical equation set and numerical solution methods are correctly implemented and appropriate to the widely used neutronic application ARCADIA® code system methodology. In addition, benchmarking results were found to be suitable for application to neutronic design analyses of pressurized water reactors. Thus, based on the technical evaluation above, the NRC staff finds the ARCADIA® code system methodology for PWRs acceptable for licensing applications subject to the Limitations and Conditions specified in Section 3.0 of this SE.

5.0 REFERENCES

1. ANP-10297P, Revision 0, “The ARCADIA® Reactor Analysis System for PWRs Methodology Description and Benchmarking Results,” March 30, 2010, ADAMS Accession No. ML100950584.

2. ANP-10297Q1P, Revision 1, “Response to Requests for Additional Information for the Review of the ARCADIA® Reactor Analysis System for PWRs Methodology Description and Benchmarking Results Topical Report,” May 10, 2011, ADAMS Accession No. ML11143A107.

3. G. H. Hobson et al, “NEMO-Nodal Expansion Method Optimized,” BAW-10180-A, Revision 1, B&W Fuel Company, Lynchburg, Virginia, March 1993.

4. BAW-10288P-A, SCIENCE, December 2000.

5. “Safety Evaluation by the Office of Nuclear Reactor Regulation Related to the Review of Topical Report COBRA-FLX: A Core Thermal-Hydraulic-Analysis Code, ANP-10311P, Revision 0, TAC No. ME 3909,” March 16, 2011, ADAMS Accession No. ML110550464.

6. ANP-10311P, Revision 0, "COBRA-FLX: A Core Thermal-Hydraulic Analysis Code Topical Report," March 2010, ADAMS Accession No. ML101550172.

7. "APOLLO2-A- AREVA's New Generation Lattice Physics Code: Methodology and Validation", PHYSOR 2010, Pittsburg, Pennsylvania, USA May 9-14, 2010.

8. ANSI/ANS-19.6.1-2005, "Reload Startup Physics Tests for Pressurized Water Reactors," American Nuclear Society, 2005.

9. "Urania Gadolinia: Nuclear Model Development and Critical Experiment 11 Benchmark," BAW-1810, April 1984.

10. H. Finnemann, H. Bauer, A. G. Galati, and R. Martinelli, "Results of LWR Core Transient Benchmarks," NEA/NSC/DOC(93)25, October 1993.

11. P. K. Hutt, and M. P. Knight, "The Development of a Transient Neutron Flux Solution in the PANTHER Code," Transactions of the American. Nuclear Society, 61, 348, 1990.

12. L. W. Newman et al., "Urania Gadolinia: Nuclear Model Development and Critical Experiment Benchmark," DOE/ET/34212-41, BAW-1810, April 1984.

13. G. H. Hobson et al, "NEMO-Nodal Expansion Method Optimized," BAW-10180-A, Revision 1, B&W Fuel Company, Lynchburg, Virginia, March 1993.

14. EMF-93-164(P)(A), "Power Distribution Measurement Uncertainty For INPAX-W in Westinghouse Plants," February 1, 1995, ADAMS Accession No. ML102030175.

15. EMF-96-029(P)(A), "Reactor Analysis System for PWRs," May 1, 1996.

16. ANP-10287-P-A, "Incore Trip Setpoint and Transient Methodology for the U.S. EPR TR," November 30, 2007.

Principal Contributors: A. Attard
A. K. Heller

Date: February 13, 2013